



## Decadal change in the relationship between the oceanic entrainment temperature and thermocline depth in the far western tropical Pacific

Rong-Hua Zhang,<sup>1</sup> Antonio J. Busalacchi,<sup>1</sup> and Yan Xue<sup>2</sup>

Received 21 September 2007; revised 6 November 2007; accepted 13 November 2007; published 8 December 2007.

[1] The interaction between the thermocline and mixed layer is a key process important to the El Niño-Southern Oscillation (ENSO) in the tropical Pacific climate system. Decadal changes in the relationships between the depth of 20°C isotherm ( $D_{20C}$ ) and the temperature of subsurface water entrained into the mixed layer ( $T_e$ ) are analyzed using observed temperature data during the periods 1955–2003 in association with the 1976–77 climate shift. The thermocline in the western tropical Pacific is anomalously deep before the shift, but shallow after the shift. It is found that the relationship has undergone decadal change in the far western tropical Pacific (west of 160°E). The effects of the decadal changes in the  $D_{20C}$ - $T_e$  relationships on ENSO properties are further examined using an intermediate coupled model (ICM). It is demonstrated that ENSO properties are sensitive to the decadal changes in the  $D_{20C}$ - $T_e$  relationship in the far western tropical Pacific. **Citation:** Zhang, R.-H., A. J. Busalacchi, and Y. Xue (2007), Decadal change in the relationship between the oceanic entrainment temperature and thermocline depth in the far western tropical Pacific, *Geophys. Res. Lett.*, *34*, L23612, doi:10.1029/2007GL032119.

### 1. Introduction

[2] El Niño has undergone decadal changes in its properties in association with the so-called 1976–77 climate shift [e.g., Rasmusson and Carpenter, 1982; Miller *et al.*, 1994; Kirtman and Schopf, 1998; Fedorov and Philander, 2000; Zhang and Busalacchi, 2005]. In particular, decadal changes in the onset locations of El Niño-related SST anomalies and their subsequent propagation directions took place in the late 1970s. What processes are responsible for the decadal changes in the onset locations of El Niño-related SST anomalies? Various mechanisms have been proposed that may contribute to the decadal modulations of ENSO in the late 1970s. They include stochastic forcing in the atmosphere, subtropical cells (STCs), changes in the mean climate states in the tropics, and changes in the surface wind structure [e.g., Kirtman and Schopf, 1998; Kleeman *et al.*, 1999; Fedorov and Philander, 2000; Wang and An, 2001].

[3] As an interface field between the thermocline and mixed layer,  $T_e$  is an important variable to large-scale air-sea interactions in the tropics. It was first recognized more

than a decade ago that ENSO variability is very sensitive to the entrainment temperature parameterization in the tropical Pacific climate system [e.g., Zebiak and Cane, 1987]. In many subsequent studies, the role of  $T_e$  in ENSO physics and variability have been clearly demonstrated. More recently, Zhang and Busalacchi [2005] have identified  $T_e$  as an important factor for decadal changes in ENSO properties using an ICM. In particular, this simplified modeling study, utilizing an empirical  $T_e$  parameterization constructed from historical data during the pre- and post-shift periods, provides a specific explanation for decadal changes in the structure of ENSO as observed in the late 1970s.

[4] Here we will use observed temperature data to analyze decadal changes in the structure and amplitude of  $T_e$  variability and its relationship with thermocline variability. Previously, the relationship between the thermocline and SST have been examined mostly on interannual time scales associated with ENSO [e.g., Zelle *et al.*, 2004]; the role of atmospheric winds in the western tropical Pacific in ENSO physics has also been examined quite extensively [e.g., Weisberg and Wang, 1997; Wang *et al.*, 1999; Solomon and Jin, 2005]. Our focus in this paper will be on the oceanic role of the western tropical Pacific in decadal modulations of ENSO relevant to the 1976–77 climate shift. We continue to investigate the thermocline/mixed-layer coupling since it has still received relatively little attention compared to the SST-wind coupling.

### 2. Observational Data

[5] We use upper ocean temperature observations compiled by the Joint Environmental Data Analysis Center (JEDAC)/Scripps Institution of Oceanography [White and Bernstein, 1979], whose details can be found at [http://coaac.ucsd.edu/DATA\\_IMAGES/index.html](http://coaac.ucsd.edu/DATA_IMAGES/index.html). The monthly temperature fields are available vertically at depths of 0, 20, 40, 60, 80, 120, 160, 200, 240, 300, and 400 meters, and horizontally at resolution of 5° in longitude and 2° in latitude during the periods from 1955 to 2003.

[6] Temperature-based mixed layer (ML) depth is first obtained as the depth at which the temperature is 0.5° below SST; its long-term annual mean field is shown in Figure 1a. Using this definition, however, means that  $T_e$  is always equal to SST-0.5°C, which is not necessary. To avoid this, we define  $T_e$  at depth:  $h_m = h_m^{SST-0.5} + 10$ . Correspondingly,  $T_e$  is estimated as the temperature at the depth of 10 meters below the depth where the temperature is 0.5° less than SST. The temperature fields are also used to calculate the depth of the thermocline (defined as the 20°C isotherm depth;  $D_{20C}$ ), which is estimated simply by linear interpolation from the two nearest depths. The obtained  $T_e$  and  $D_{20C}$  anomaly fields are horizontally interpolated to the ICM grid

<sup>1</sup>Earth System Science Interdisciplinary Center, University of Maryland at College Park, Maryland, USA.

<sup>2</sup>Climate Prediction Center, National Centers for Environmental Prediction, National Weather Service, NOAA, Camp Springs, Maryland, USA.

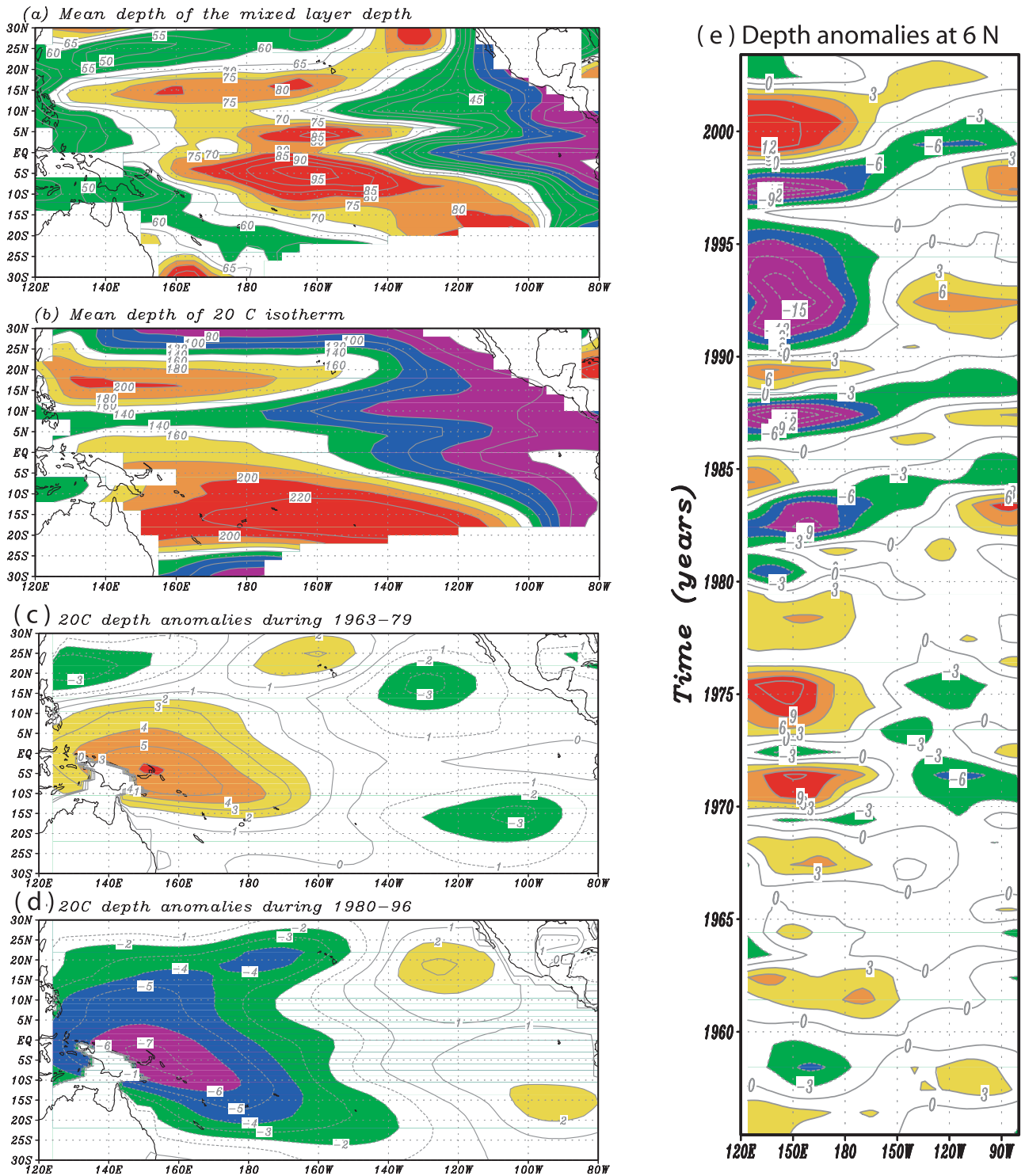


**Figure 1.** Horizontal structure of the (a) mean depth of the mixed layer and (b) 20°C isotherm ( $D_{20C}$ ) estimated from the JEDAC data during the periods 1955–2003. Horizontal distribution of  $D_{20C}$  anomalies estimated separately for the two subperiods (c) 1963–1979 and (d) 1980–1996. (e) Interannual  $D_{20C}$  anomalies along 6°N from 1955 to 2003 which are plotted using their yearly mean fields. The contour interval is 5 m in Figure 1a, 20 meters in Figure 1b, 1 meter in Figures 1c and 1d, and 3 m in Figure 1e.

[Zhang and Busalacchi, 2005] for the analyses shown below.

[7] At present, the determinations of entrainment temperature into the ML is a great challenge since the details of the

temperature, salinity and density structure at subsurface depth and the ML-thermocline interactions are not known well due to a lack of high resolution observations. For example, it is well known that in the western Pacific salinity

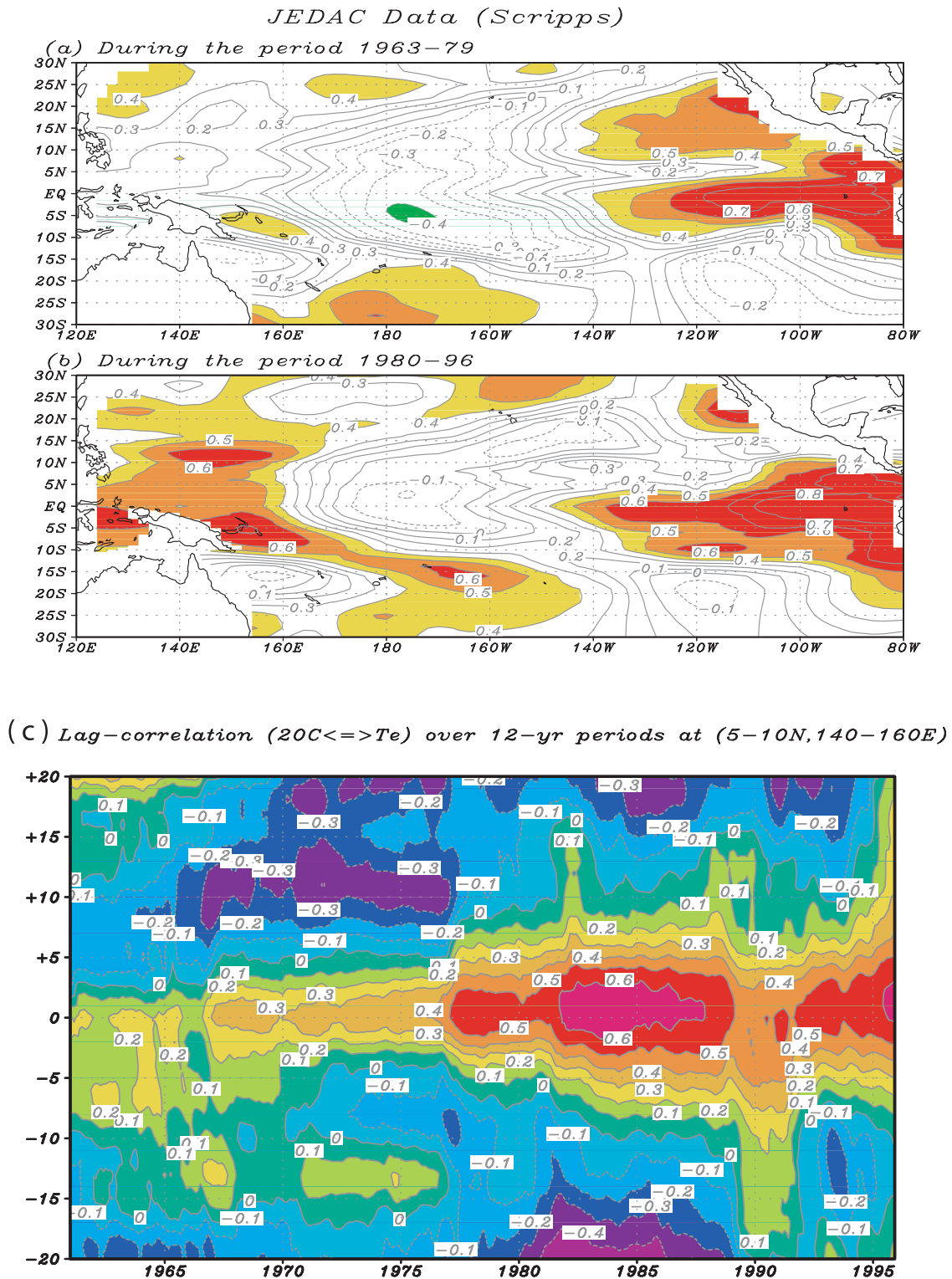


**Figure 2.** Correlations between  $T_e$  and  $D_{20C}$  anomalies calculated separately for the two subperiods (a) 1963–1979 and (b) 1980–1996. (c) Lag-correlations between the  $T_e$  and  $D_{20C}$  anomalies in the Niño6\_S region (140°E–160°E, 5°N–10°N) computed using a 12-year running window during the periods 1955 to 2003. In Figure 2c, the  $D_{20C}$  anomaly time series is chosen as a reference, with negative lags referring to a lead by  $D_{20C}$  and positive lags referring to a lead by  $T_e$ . The contour interval is 0.1.

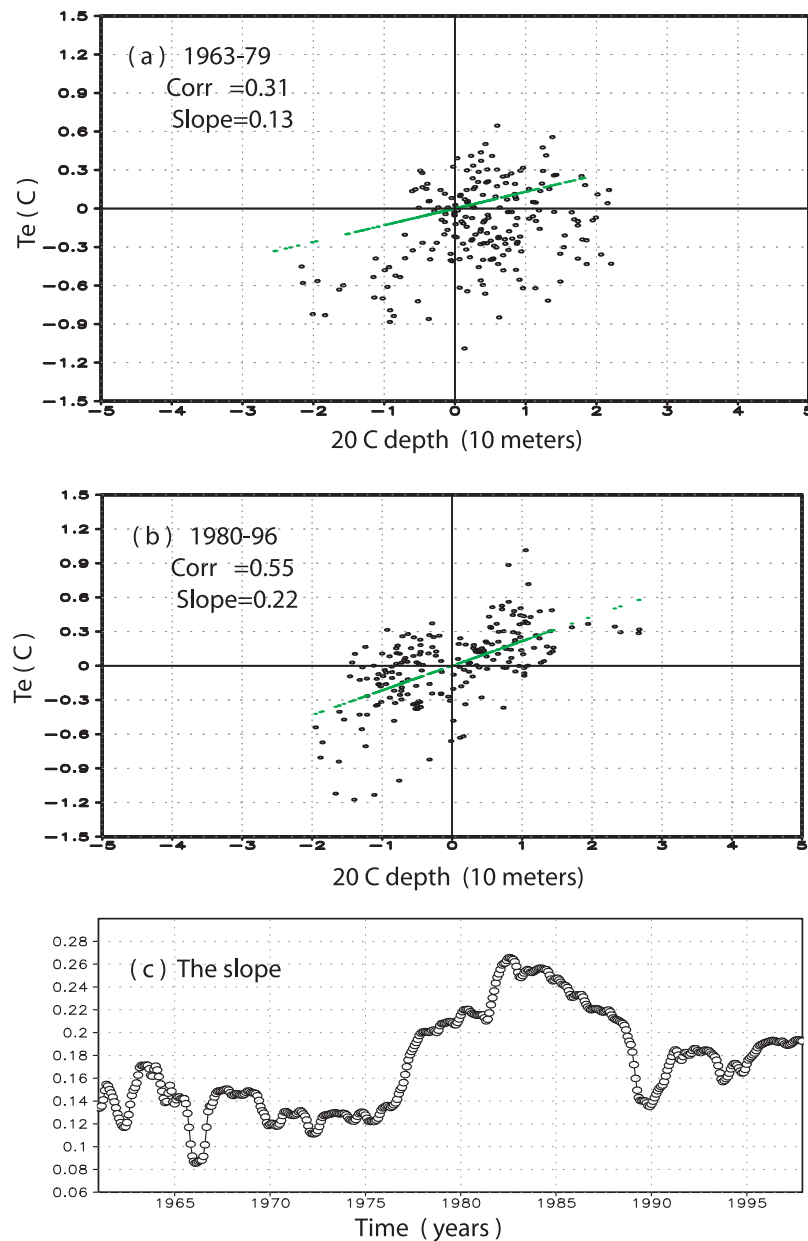


**Figure 3.** Scatterplots for the  $T_e$  and  $D_{20C}$  anomalies averaged in the Niño6\_S region separately illustrated during the two subperiods (a) 1963–1979 and (b) 1980–1996; and (c) the temporal evolution of the slope for the  $T_e$  and  $D_{20C}$  anomalies (°C per 10 meters) averaged in the Niño6\_S region using a 12-year sliding window during the periods from 1961 to 1997.

plays an important role in determining ML depth and there is often a barrier layer in which the base of the ML is controlled by salinity rather than temperature. Since sufficient salinity data are not available, in the present paper, the ML depth is estimated by the temperature difference relative to the surface, and  $T_e$  is simply estimated based on temperature profiles alone. These choices are rather arbitrary indeed.

### 3. Decadal Changes in the Relationships Between $D_{20C}$ and $T_e$ Anomalies

[8] Figure 1b shows the long-term mean depth of 20°C isotherm ( $D_{20C}$ ) estimated during the periods 1955–2003

from the JEDAC data. Some unique features of the mean thermocline structure are evident in the tropical Pacific. In particular, the thermocline is shallow along 5–10°N in the western tropical Pacific. Following *Weisberg and Wang* [1997] who define a new index, called Niño6, for the west-northern tropical Pacific, we use its southern subregion Niño6\_S (140°E–160°E and 5°N–10°N). The thermocline is shallow in the Niño6\_S region: on average, it is less than 140 meters; seasonally, it is shallowest in December (about 122 m) and deepest in April (about 146 m), respectively.

[9] Significant changes in the upper ocean thermal structure took place in the tropical Pacific Ocean in the late 1970s [e.g., *Zhang et al.*, 1998], which is clearly manifested

in the  $D_{20C}$  field (Figures 1c, 1d, and 1e). Corresponding to the climate shift, the thermocline is anomalously deep in the west during the period 1963–79 (Figure 1c), but shallow during the period 1980–1996 (Figure 1d). Horizontally, the decadal change is more pronounced in the west, while it is not significant in the east (Figures 1c and 1d). Off the equator along  $6^\circ\text{N}$  where the mean depth of the thermocline is shallow, there are large decadal  $D_{20C}$  changes as well (Figure 1e). So, taking the mean thermocline depth and seasonal and decadal fluctuations into consideration together, the thermocline can be as shallow as 110 meter in the Niño6\_S region during the early winter season.

[10] Since the thermocline is a major source for  $T_e$  variability in the tropical Pacific, decadal changes in  $D_{20C}$  are manifested in  $T_e$ . As shown by Zhang and Busalacchi [2005], the  $T_e$  anomaly fields indeed exhibit decadal changes that took place in the late 1970s, with pronounced differences in the spatial structure and amplitude of  $T_e$  variability that are relevant to the modulation of ENSO. In particular, there are noticeable decadal changes in the strength of  $T_e$  variability in the off-equatorial western Pacific along  $6$ – $10^\circ\text{N}$ . During the pre-shift period,  $T_e$  anomalies are relatively weak. After the late 1970s,  $T_e$  anomalies are much larger and are more tightly connected to the thermocline variability.

[11] The relationship between the thermocline depth and  $T_e$  in the tropical Pacific is illustrated in Figure 2 showing the correlations between  $T_e$  and  $D_{20C}$  anomalies calculated separately during the two subperiods 1963–1979 and 1980–1996, respectively. It is well known that these two fields are well correlated in the eastern equatorial Pacific as demonstrated in singular value decomposition (SVD) analysis [e.g., Zhang and Busalacchi, 2005]. A major finding from this study is that the relationships between  $D_{20C}$  and  $T_e$  variability have decadal fluctuations in the far western tropical Pacific (west of  $165^\circ\text{E}$ ). It is striking that  $T_e$  and  $D_{20C}$  anomalies are highly correlated in Niño6\_S regions after the shift (the correlations are over 0.55) while the correlations are low before the shift. Figures 3a and 3b show the scatterplot for  $T_e$  and  $D_{20C}$  anomalies illustrating the relationship separately for the two subperiods 1963–1979 and 1980–1996. A good correspondence exists between the two fields in the Niño6\_S region in the later period, with positive (negative)  $T_e$  anomalies mostly accompanied by positive (negative)  $D_{20C}$  anomalies. To obtain a temporal evolution of the relationships between  $T_e$  and  $D_{20C}$  anomalies, their lag-correlations in the Niño6\_S region are computed using a 12-year running window for the periods from 1955 to 2003 (Figure 2c). The time series of the correlations exhibits decadal changes, with a sudden increase of the correlations in the late 1970s and keeping higher in the 1980s and 1990s. It is noticed that  $D_{20C}$  and  $T_e$  variability is largely in phase.

[12] The decadal changes in the relationship between the  $D_{20C}$  and  $T_e$  variability can be further estimated by a regression analysis from the observed data, i.e., the slope of  $T_e/D_{20C}$  defined as the covariance of  $T_e$  and  $D_{20C}$  anomalies divided by the standard deviation of  $D_{20C}$  anomalies. As already indicated in Figure 3, the estimated slope in the Niño6\_S region is about  $0.13^\circ\text{C}$  per 10 m during the period 1963–1979, but it is about  $0.22^\circ\text{C}$  per 10 m during the period 1980–1996. Thus, the slope is

almost doubled. As a result, given the same depth anomaly, the amplitude of the  $T_e$  variability related by the thermocline anomalies can be significantly larger after the late 1970s. The temporal evolution of the slope for the observed  $T_e$  and  $D_{20C}$  anomalies can also be obtained using a 12-year sliding window in the Niño6\_S region (Figure 3c). Clearly, the  $T_e/D_{20C}$  slope has decadal changes as well, with significant increase in the late 1970s associated with the climate shift.

[13] We have also used other ways to estimate the ML depth and calculated the corresponding  $T_e$  fields, including a density criterion from Monterey and Levitus [1997]. Since interannual temperature anomalies in upper 100 meters are quite coherent in the western tropical Pacific, the correlation/regression patterns obtained are very similar when using different depth of the ML, indicating the results are not sensitive to the choice of the ML depth. In addition, in the western Pacific the data coverage in the Niño6\_S region is poor before the late 1960s and the decadal change in the  $T_e$ - $D_{20C}$  correlation in mid 1970s is also around the time when XBTs became much more widely used. Thus, the observed decadal transition may be reflected by the amount of data. To test this, we have examined other ocean reanalysis data, including the updated SODA products (<http://www.atmos.umd.edu>) and the global ocean reanalysis product at NCEP (GODAS; <http://www.cpc.ncep.noaa.gov/products/GODAS>). Similar results are obtained. So the results presented above from the SCRIPPS JEDAC data are robust.

#### 4. Impact on ENSO Properties: ICM Experiments

[14] After the climate shift, the effect of the thermocline on  $T_e$  in the far western tropical Pacific has been significantly enhanced as manifested in the  $T_e$ - $D_{20C}$  relationship. We hypothesize that this can modulate the way El Niño evolves. To demonstrate this, we use an intermediate coupled model (ICM; Zhang and Busalacchi [2005]), which consists of a SVD-based statistical wind stress ( $\tau$ ) model and an intermediate ocean model [Keenlyside and Kleeman, 2002] with an empirical parameterization for  $T_e$ . The relationship between the thermocline and entrainment temperature can be simply written as:

$$T_e' = \alpha_{T_e} F(D_{20C}')$$

where  $\alpha_{T_e}$  can be called the thermocline coupling coefficient representing the strength of the thermocline effect on  $T_e$ , and  $F$  refers to a spatial pattern defined by a SVD analysis [Zhang and Busalacchi, 2005]. By changing the value of  $\alpha_{T_e}$ , the amplitude of  $T_e$  anomalies calculated from the empirical  $T_e$  model can be modified before being used in the SST calculation (previously, the effects of the coupling strength between wind stress and SST on ENSO have been examined extensively). In our empirical approach to  $T_e$ , the relationships between  $T_e$  and  $D_{20C}$  variability ( $F$ ) are represented in the spatial structure of the SVD modes derived from historical data [Zhang and Busalacchi, 2005]. Previous studies have demonstrated that the decadal changes in the  $T_e$ - $D_{20C}$  relationships can be responsible for changes in the phase propagation of ENSO [Zhang and

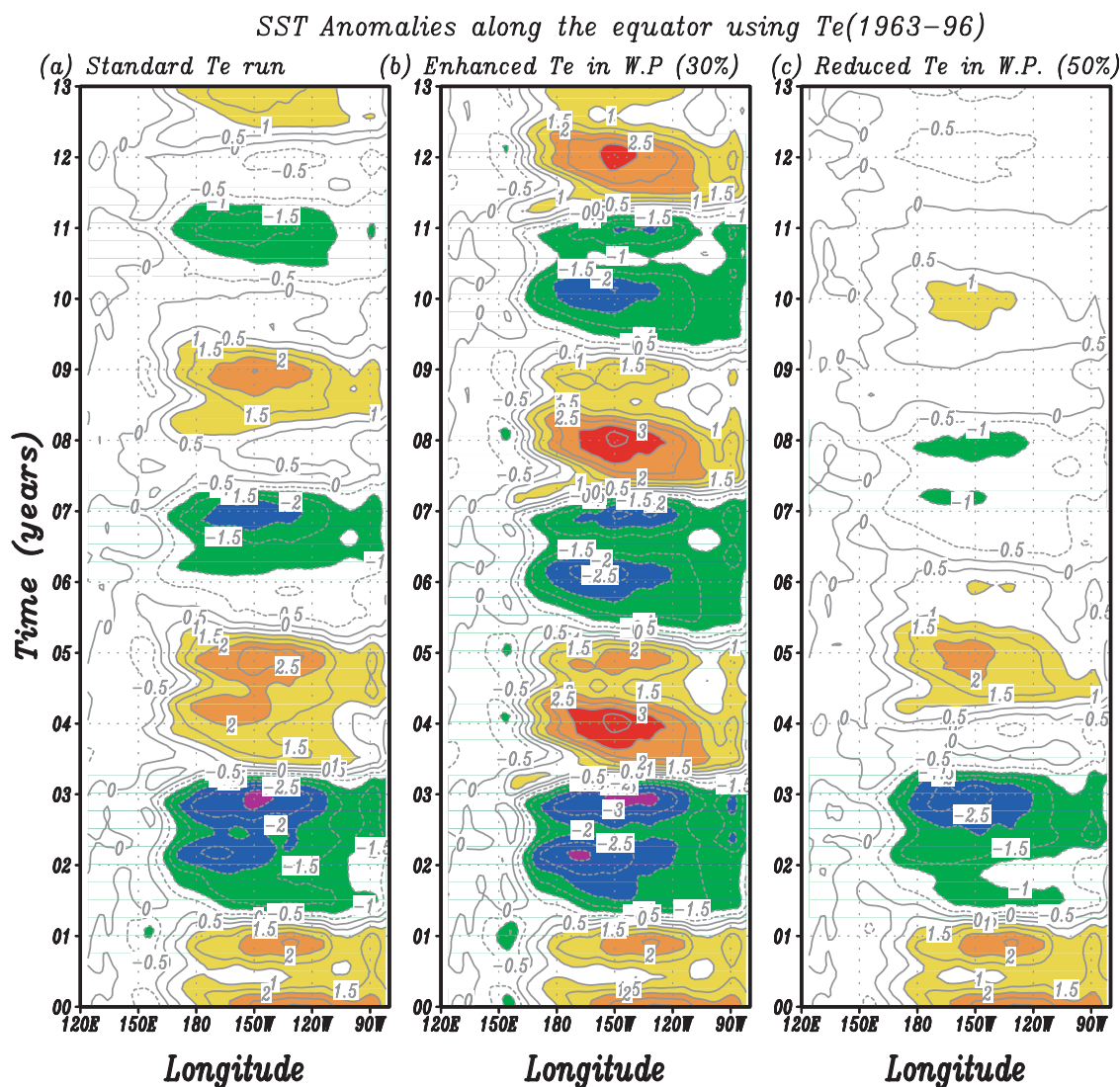


**Figure 4.** Temporal evolution of SST anomalies along the equator from ICM experiments (a) with the standard  $T_e^{63-96}$  specification (the control run); (b) with the  $T_e$  anomaly amplitude in the far western tropical Pacific increased by 30% (a stronger  $D_{20C}/T_e$  coupling run); and (c) reduced by 50% (a weaker  $D_{20C}/T_e$  coupling run). The contour interval is  $0.5^\circ\text{C}$ .

Busalacchi, 2005]. Here we will emphasize the effect on ENSO of the decadal changes in the  $D_{20C}$ - $T_e$  relationship in the far western tropical Pacific.

[15] A standard experiment is performed using the  $T_e^{63-96}$  specification (and the simulated interannual variability was presented by Zhang and Busalacchi [2005]). Sensitivity experiments are then performed by modifying the value of  $\alpha_{T_e}$  in the far western tropical Pacific *only* in order to examine the effect of an enhanced or weakened thermocline/ $T_e$  coupling on ENSO behaviors. That is, in the coupled model runs,  $\alpha_{T_e}$  is modified *only* over the far western tropical Pacific from  $140^\circ\text{E}$  to  $160^\circ\text{E}$ , with its value linearly approaching to  $1.0$  at  $180^\circ$  to the east and  $130^\circ\text{E}$  to the west, respectively.

[16] Figure 4 shows the temporal evolution of SST anomalies along the equator from the ICM experiments with the standard  $T_e^{63-96}$  specification (control run), and with the value of  $\alpha_{T_e}$  in the far western tropical Pacific increased

by 30% ( $\alpha_{T_e} = 1.3$ ; a stronger  $D_{20C}/T_e$  coupling run) and reduced by 50% ( $\alpha_{T_e} = 0.5$ ; a weaker  $D_{20C}/T_e$  coupling run), respectively. Note that the induced changes in  $\alpha_{T_e}$  in the western tropical Pacific (from  $0.5$  up to  $1.3$ ) is consistent with observed decadal changes in the  $T_e$ - $D_{20C}$  relationship in the late 1970s, as represented by regression analysis shown above (Figure 3). It turns out that modifying the strength of the  $T_e$ - $D_{20C}$  relationships in the far western Pacific *only* can modulate ENSO properties significantly. By increasing the value of  $\alpha_{T_e}$  (and so the thermocline effect on SST is stronger through enhancing the  $T_e$ - $D_{20C}$  relationship in the far western tropical Pacific), El Niño amplitude increases significantly while oscillation periods decrease slightly (Figure 4b). On the other hand, if the relationship is getting weaker, the El Niño amplitude is decreased, with a longer oscillation period (Figure 4c). The standard deviation of Niño3 SST anomalies is  $1.1^\circ\text{C}$  in the standard run, while it is  $0.8^\circ\text{C}$  in the weaker  $D_{20C}$ - $T_e$

coupling run and  $1.4^\circ\text{C}$  in the stronger  $D_{20C}$ - $T_e$  coupling run, respectively.

[17] Thus ENSO is sensitive to the amplitude of  $\alpha_{T_e}$  in the far western tropical Pacific, an indicator of the  $T_e$ - $D_{20C}$  relationship. Further experiments in which the modification of  $\alpha_{T_e}$  amplitude is restricted respectively to the off-equatorial region between  $5^\circ\text{N}$ – $15^\circ\text{N}$  and the equatorial region between  $5^\circ\text{N}$ – $5^\circ\text{S}$  indicate that the two regions make almost an equal contribution to the modulation of ENSO characteristic shown in Figure 4.

## 5. Discussion and Conclusion

[18] Observed temperature data are used to describe decadal changes in the relationships between the  $D_{20C}$  and  $T_e$  anomalies during the periods 1955–2003. A new feature is identified that may affect SST evolution and explain the decadal modulation of ENSO relevant to the climate shift in the late 1970s. It is found that the relationships between  $T_e$  and thermocline variability has undergone decadal changes. After the shift, the thermocline in the western tropical Pacific is anomalously shallow and these two fields are significantly correlated west of  $160^\circ\text{E}$ . The  $T_e/D_{20C}$  slope has been almost doubled in the far western tropical Pacific. Thus, for the same magnitude of a given  $D_{20C}$  anomaly, a larger  $T_e$  anomaly can be related to the thermocline variability, which enhances the efficiency of subsurface variability in generating SST anomalies in the west. An ICM of the tropical Pacific climate system is used to demonstrate the effects of the decadal changes in the  $D_{20C}$ - $T_e$  relationship on El Niño evolution. Simply through modifying the coupling strength between the  $D_{20C}$  and  $T_e$  anomalies in the far western tropical Pacific *only*, significant effect on the El Niño amplitude is found. An increase of 30% in the thermocline effect on  $T_e$  in the far western tropical Pacific ( $140^\circ\text{E}$ – $160^\circ\text{E}$ ) corresponds to a 27% increase in the Niño3 standard deviation (from  $1.1^\circ\text{C}$  to  $1.4^\circ\text{C}$ ), and a more pronounced SST anomaly pattern along the NECC pathway in the west. Thus, the far western tropical Pacific can be an important region for modulating ENSO variability. Clearly, the  $T_e/D_{20C}$  relationship in the far western tropical Pacific is not stationary and appears to be modulated by interdecadal variability in the thermocline depth which is affected by tropical-extratropical interactions in the western Pacific, a topic that needs to be examined further.

[19] **Acknowledgments.** We would like to thank A. Wittenberg, P. Schopf, B. Kirtman, Z. Liu, F.-F. Jin for their comments. The authors wish to thank anonymous reviewers for their numerous comments. This research is supported in part by NASA grants (NCC5374 and NAG512246) and NSF ATM-0727668.

## References

- Fedorov, A. V., and S. G. H. Philander (2000), Is El Niño changing?, *Science*, *228*, 1997–2002.
- Keenlyside, N., and R. Kleeman (2002), Annual cycle of equatorial zonal currents in the Pacific, *J. Geophys. Res.*, *107*(C8), 3093, doi:10.1029/2000JC000711.
- Kirtman, B. P., and P. S. Schopf (1998), Decadal variability in ENSO predictability and prediction, *J. Clim.*, *11*, 2804–2822.
- Kleeman, R., J. P. McCreary, and B. A. Klinger (1999), A mechanism for generating ENSO decadal variability, *Geophys. Res. Lett.*, *26*, 1743–1746.
- Miller, A. J., D. R. Cayan, T. P. Barnett, N. E. Graham, and J. M. Oberhuber (1994), The 1976–77 climate shift of the Pacific Ocean, *Oceanography*, *7*, 21–26.
- Monterey, G., and S. Levitus (1997), Seasonal variability of mixed layer depth for the World Ocean, *NOAA Atlas NESDIS 14*, 96 pp., U.S. Gov. Print. Off., Washington, D. C.
- Rasmusson, E. M., and T. H. Carpenter (1982), Variations in tropical sea surface temperature and surface wind fields associated with the Southern Oscillation/El Niño, *Mon. Weather Rev.*, *110*, 354–384.
- Solomon, A., and F.-F. Jin (2005), A study of the impact of off-equatorial warm pool SST anomalies on ENSO cycles, *J. Clim.*, *18*, 274–286.
- Wang, B., and S.-I. An (2001), Why the properties of El Niño changed during the late 1970s, *Geophys. Res. Lett.*, *28*, 3709–3712.
- Wang, B., R. Wu, and R. Lukas (1999), Roles of the western North Pacific wind variation in thermocline adjustment and ENSO phase transition, *J. Meteorol. Soc. Jpn.*, *77*, 1–16.
- Weisberg, R. H., and C. Wang (1997), A western Pacific oscillator paradigm for the El Niño-Southern Oscillation, *Geophys. Res. Lett.*, *24*, 779–782, doi:10.1029/97GL00689.
- White, W. B., and R. L. Bernstein (1979), Design of an oceanographic network in the mid-latitude North Pacific, *J. Phys. Oceanogr.*, *9*, 592–606.
- Zebiak, S. E., and M. A. Cane (1987), A model El Niño/Southern Oscillation, *Mon. Weather Rev.*, *115*, 2262–2278.
- Zelle, H., G. Appeldoorn, G. Burgers, and G. J. van Oldenborgh (2004), The relationship between sea surface temperature and thermocline depth in the eastern equatorial Pacific, *J. Phys. Oceanogr.*, *34*, 643–655.
- Zhang, R.-H., and A. J. Busalacchi (2005), Interdecadal changes in properties of El Niño in an intermediate coupled model, *J. Clim.*, *18*, 1369–1380.
- Zhang, R.-H., L. M. Rothstein, and A. J. Busalacchi (1998), Origin of upper-ocean warming and El Niño change on decadal scale in the tropical Pacific Ocean, *Nature*, *391*, 879–883.

A. J. Busalacchi and R.-H. Zhang, Earth System Science Interdisciplinary Center, University of Maryland at College Park, Computer and Space Science Building, Room 2231, College Park, MD 20742, USA. (rzhang@essic.umd.edu)

Y. Xue, Climate Prediction Center, NCEP, NWS, NOAA, 5200 Auth Road, Room 605-A, WWB, Camp Springs, MD 20746, USA.